with a dielectric constant of 1 and with a nonbonded cut-off range of 15 Å, with a switch function operating from 11 to 14 Å. For the final energy minimization the Ewald summation with a cut-off of 20 Å for nonbonding interactions was used. Electrostatic point charges were taken from templates provided by QUANTA. For the generation of a systematic search a charmm script was written, which is an implementation of the cluster search method of Gavezotti[15] but limited to translational symmetry operations. Each search started with a different conformation of the bisurea compound, and gave 5–10 trial structures. These trial structures were then energy minimized to an energy gradient of 0.00005.

Received: August 28, 1998
Revised version: February 15, 1999 [Z 12347 IE]
German version: *Angew. Chem.* **1999**, *111*, 1486–1490

**Keywords:** conducting materials · gels · microwave conductivity · supramolecular chemistry

[1] a) A. Dodabalapur, L. Torsi, H. E. Katz, *Science* **1995**, *268*, 270–271; b) G. Horowitz, *Adv. Mater.* **1998**, *10*, 365–377; c) Z. Bao, A. Lovinger, J. Brown, *J. Am. Chem. Soc.* **1998**, *120*, 207–208.
[2] a) J. H. Burroughes, D. D. C. Bradley, A. R. Brown, R. N. Marks, K. Mackay, R. H. Friend, P. L. Burns, A. B. Holmes, *Nature* **1990**, *347*, 539–541; b) F. Geiger, M. Stoldt, H. Schweizer, P. Bäuerle, E. Umbach, *Adv. Mat*er. **1993**, *5*, 922–925.
[3] M. Pope, C. E. Swenberg, *Electronic Processes in Organic Crystals*, Oxford University Press, New York, **1982**.
[4] a) A. Kraft, A. C. Grimsdale, A. B. Holmes, *Angew. Chem.* **1998**, *110*, 416–443; *Angew. Chem. Int. Ed.* **1998**, *37*, 402–428; b) X.-C. Li, H. Sirringhaus, F. Garnier, A. B. Holmes, S. C. Moratti, N. Feeder, W. Clegg, S. J. Teat, R. H. Friend, *J. Am. Chem. Soc.* **1998**, *120*, 2206–2207.
[5] a) T. Siegrist, C. Kloc, R. A. Laudise, H. Katz, R. C. Haddon, *Adv. Mater.* **1998**, *10*, 379–383; b) R. Hajlaoui, D. Fichou, G. Horowitz, B. Nessakh, M. Constant, F. Garnier, *Adv. Mater.* **1997**, *9*, 557–561; c) Z. Bao, A. Dodabalapur, A. J. Lovinger, *Appl. Phys. Lett.* **1996**, *69*, 4108–4110; d) for a recent example of polythiophenes, see T. Bjørnholm, D. R. Greve, N. Reitzel, T. Hassenkam, K. Kjaer, P. B. Howes, N. B. larsen, J. Bøgelund, M. Jayaraman, P. C. Ewbank, R. D. McCullough, *J. Am. Chem. Soc.* **1998**, *120*, 7643–7644.
[6] a) G. R. Desiraju, *Crystal Engineering: The Design of Organic solids*, Elsevier, Amsterdam, **1989**; G. R. Desiraju, *Angew. Chem.* **1995**, *107*, 2541–2558; *Angew. Chem. Int. Ed. Engl.* **1995**, *34*, 2311–2327; b) J. C. MacDonald, G. M. Whitesides, *Chem. Rev.* **1994**, *94*, 2383–2420.
[7] a) F. D. Lewis, J.-S. Yang, C. L. Stern, *J. Am. Chem. Soc.* **1996**, *118*, 2772–2773; b) H. Bock, W. Seitz, M. Sievert, M. Kleine, J. W. Bats, *Angew. Chem.* **1996**, *108*, 2382–2384; *Angew. Chem. Int. Ed. Engl.* **1996**, *35*, 2244–2246; c) C. L. Schauer, E. Matwey, F. W. Fowler, J. W. Lauher, *J. Am. Chem. Soc.* **1997**, *119*, 10245–10246.
[8] a) X. Zhao, Y. L. Chang, F. W. Fowler, J. W. Lauher, *J. Am. Chem. Soc.* **1990**, *112*, 6627–6634; b) M. C. Etter, Z. Urbańczyk-Lipkowska, M. Zia-Ebrahimi, T. W. Panunto, *J. Am. Chem. Soc.* **1990**, *112*, 8415–8426; c) M. D. Hollingsworth, M. E. Brown, B. D. Santarsiero, J. C. Huffman, C. R. Ross, *Chem. Mater.* **1994**, *6*, 1227–1244; d) J. J. Kane, R.-F. Liao, J. W. Lauer, F. W. Fowler, *J. Am. Chem. Soc.* **1995**, *117*, 12003–12004; e) M. de Loos, J. van Esch, I. Stokroos, R. M. Kellogg, B. L. Feringa, *J. Am. Chem. Soc.* **1997**, *119*, 12675–12676.
[9] a) J. van Esch, R. M. Kellogg, B. L. Feringa, *Tetrahedron Lett.* **1997**, *38*, 281–284; b) J. van Esch, S. De Feyter, R. M. Kellogg, F. De Schryver, B. L. Feringa, *Chem. Eur. J.* **1997**, *3*, 1238–1243.
[10] a) P. Terech, R. G. Weiss, *Chem. Rev.* **1997**, *97*, 3133–3159; b) K. Hanabusa, K. Shimura, K. Hirose, M. Kimura, H. Shirai, *Chem. Lett.* **1996**, 885–886.
[11] a) Y. Mido, *Spectrochim. Acta A* **1973**, *29*, 431–438; b) J. Jadzyn, M. Stockhausen, B. Zywucki, *J. Phys. Chem.* **1987**, *91*, 754–757.
[12] a) R. Kasha, H. R. Rawls, M. Asraf El-Bayoumi, *Pure Appl. Chem.* **1965**, *11*, 371–392; b) V. Czikklely, H. D. Försterling, H. Kuhn, *Chem. Phys. Lett.* **1970**, *6*, 11–14; c) V. Czikklely, H. D. Försterling, H. Kuhn, *Chem. Phys. Lett.* **1970**, *6*, 207–210.
[13] O. Wörz, G. Scheibe, *Z. Naturforsch. B* **1969**, *24*, 381.
[14] M. Rubio, M. Merchán, E. Ortí, B. Roos, *J. Phys. Chem.* **1995**, *102*, 3580–3586, and references therein.
[15] A. Gavezotti, *J. Am. Chem. Soc.* **1991**, *113*, 4622–4629.
[16] B. R. Brooks, R. E. Bruccoleri, D. B. Olafson, D. J. States, S. Swaminathan, M. Karplus, *J. Comput. Chem.* **1983**, *4*, 187–217.
[17] J. M. Warman, M. P. de Haas in *Pulse-Radiolysis* (Ed.: Y. Tabata), CRC, Boca Raton, FL, USA, **1991**, p. 101.
[18] M. P. de Haas, G. P. van der Laan, B. Wegewijs, D. M. de Leeuw, P. Bäuerle, D. B. A. Rep, D. Fichou, *Synth. Met.*, in press.
[19] G. P. van der Laan, M. P. de Haas, A. Buik, B. de Ruiter, *Synth. Met.* **1993**, *55–57*, 4930.

# Fast Experiments for Charge-Density Determination: Topological Analysis and Electrostatic Potential of the Amino Acids L-Asn, DL-Glu, DL-Ser, and L-Thr**

Ralf Flaig, Tibor Koritsánszky, Jan Janczak, Hans-Georg Krane, Wolfgang Morgenroth, and Peter Luger*

X-ray diffraction experiments not only give atomic positions from which the geometry of a chemical structure can be determined, but the exact charge density distribution $\rho(\mathbf{r})$ can also be deduced,[1] which is an observable in contrast to the wave-function in the Schrödinger equation. To accomplish this the experiment has to be carried out up to high resolution ($d \leq 0.5$ Å or $\sin\theta\,\lambda^{-1} \geq 1.0$ Å$^{-1}$) and at the lowest temperature possible. With conventional diffractometers and serial (scintillation) detection this required measurement periods of several weeks or even months, even for structures of moderate size (20–30 atoms), so that the method, although known since the 1960s,[2] was hardly applied and led only to more qualitative results. In the meantime several developments have changed the situation drastically.

By means of Bader's theory of "atoms in molecules", which was developed on a quantum chemical basis, a topological analysis of $\rho(\mathbf{r})$ allows a well-defined partitioning of a chemical structure into sub-molecular regions (atoms or functional groups).[3] This initiated the generation of appro-

[*] Prof. Dr. P. Luger, Dipl.-Chem. R. Flaig, Dr. J. Janczak
Institut für Kristallographie der Freien Universität Berlin
Takustrasse 6, D-14195 Berlin (Germany)
Fax: (+49) 30-838-3464
E-mail: luger@chemie.fu-berlin.de
Prof. Dr. T. Koritsánszky
Department of Chemistry, University of the Witwatersrand
Private Bag 3, WITS 2050, Johannesburg (South Africa)
Dr. H.-G. Krane
Mineralogisch-Petrologisches Insitut der Universität
Poppelsdorfer Schloss, D-53115 Bonn (Germany)
Dr. W. Morgenroth
Institut für Mineralogie und Petrographie der Universität
Grindelallee 48, D-20146 Hamburg (Germany)

[**] This work was funded by the BMBF (Verbund 47, Förderkennzeichen 05 SM8KEA0), the Alexander von Humboldt-Stiftung, and the Fonds der Chemischen Industrie.

priate computer programs, among them XD,[4] which is able to calculate all the properties that can be deduced from the charge density and display them as high quality graphics.

Almost at the same time experimental conditions have improved substantially, with intensive X-ray sources (especially synchrotron radiation) and low temperatures (down to 15 K) contributing to a better scattering from the sample. Thanks to the emergence of area detectors (imaging plates or CCDs) a decisive breakthrough has been accomplished and this has increased the number of reflections that could be measured per unit time by about two orders of magnitude. This reduced the measurement periods from several weeks to one or a few days.[5]

Recently we started comparative charge density determinations in the group of the 20 naturally occurring amino acids to deduce, as far as possible, their topological and electrostatic properties, and in particular to study the reproducibility and transferability in the vicinity of the $C_\alpha$-carbon atom. At the same time there is a chance to supplement Bader's theoretical works[6] and prove experimentally the transferability of electronic properties of molecular and submolecular fragments from this class of compounds onto larger systems like oligopeptides.

Herein we describe the results for L-asparagine monohydrate, DL-glutamic acid monohydrate, DL-serine, and L-threonine, which are based mainly on fast diffraction experiments performed at Hasylab/DESY with a combination of synchrotron radiation/CCD area detection[7] (Table 1). A first experiment of this kind was reported recently.[5] The synchrotron experiment with DL-serine,[8] which was executed up to a resolution of $d = 0.33$ Å ($\sin\theta\lambda^{-1} = 1.54$ Å$^{-1}$), is probably one of the most highly resolved diffraction experiments in charge density work. Further charge density studies based on conventional experiments that took several weeks are known for the amino acids L-alanine,[9] glycine,[10] DL-histidine,[11] and DL-aspartic acid.[12]

Table 1. Summary of the different measurements, experimental conditions, and figures of merit.

| | Asn | Glu | Ser (Sy) | Ser (Mo) | Thr |
|---|---|---|---|---|---|
| radiation/beamline | Sy/F1 | Sy/F1 | Sy/D3 | $Mo_{K\alpha}$/Smart | $Ag_{K\alpha}$/four circle |
| wavelength [Å] | 0.5297 | 0.5297 | 0.4500 | 0.7107 | 0.5608 |
| resolution ($d/\sin\theta\lambda^{-1}$) [Å/Å$^{-1}$] | 0.34/1.46 | 0.39/1.30 | 0.33/1.54 | 0.41/1.22 | 0.37/1.34 |
| temperature [K] | 100 | 100 | 100 | 123 | 19 |
| measurement time [d] | | | < 2 | | 25 |
| reflections | | | | | |
| total | 58720 | 59716 | 49928 | 19567 | 12215 |
| unique | 11452 | 13940 | 11120 | 6333 | 5994 |
| $F_o > 3\sigma(F_o)$ | 9972 | 9246 | 7127 | 5181 | 4487 |
| $R(F)$ | 0.0333 | 0.0455 | 0.0362 | 0.0433 | 0.0204 |
| $Rw(F)$ | 0.0266 | 0.0347 | 0.0309 | 0.0341 | 0.0167 |

Qualitative and quantitative results for the Laplacian function $\nabla^2\rho(\mathbf{r})$[13] are compiled in Figure 1 and Table 2, respectively. Since $\nabla^2\rho(\mathbf{r})$ has a finer structure than $\rho(\mathbf{r})$ small changes of the charge density that arises from bond formation

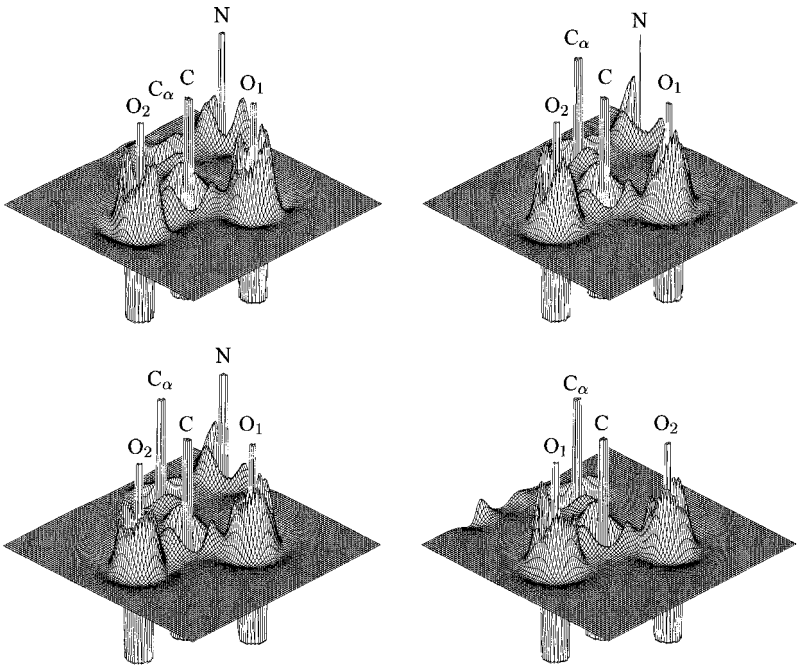


Figure 1. Relief representation of the negative Laplacian function in the plane of the carboxylate group: L-Asn (top left), DL-Glu (top right), DL-Ser (bottom left), and L-Thr (bottom right).

Table 2. Charge density [e Å$^{-3}$] (first line) and Laplacian function [e Å$^{-5}$] (second line) at the bond critical points. The two C–O bonds in the carboxylate group are distinguished by their different (partly to a small extent) bond lengths. C–O(1) corresponds to the longer and C–O(2) to the shorter bond.

| bond | Asn | Glu | Ser (Sy) | Ser (Mo) | Thr | Pro[5] | Asp[12] | Ala[9] | Gly[10] | Average |
|---|---|---|---|---|---|---|---|---|---|---|
| O(1)-C | 2.74(4) | 2.53(4) | 2.70(3) | 2.55(4) | 2.64(4) | 2.83(4) | 2.71(3) | 2.86 | 2.67 | 2.69(11) |
| | −34.3(2) | −27.3(2) | −36.1(1) | −32.0(3) | −30.7(3) | −39.3(3) | −37.6(2) | −29.6 | −30.5 | −33.0(40) |
| O(2)-C | 2.90(4) | 2.77(4) | 2.74(3) | 2.67(4) | 2.78(4) | 2.84(4) | 2.87(3) | 3.02 | 2.77 | 2.82(10) |
| | −32.5(2) | −33.9(3) | −35.7(2) | −31.4(3) | −38.1(2) | −34.3(3) | −36.1(2) | −39.0 | −32.8 | −34.9(26) |
| N-$C_\alpha$ | 1.74(3) | 1.72(3) | 1.69(2) | 1.72(3) | 1.72(3) | 1.68(2) | 1.69(2) | 1.70 | 1.69 | 1.71(2) |
| | −13.6(1) | −9.3(1) | −11.4(1) | −16.9(2) | −13.2(1) | −9.7(1) | −12.9(1) | −11.1 | −11.9 | −12.2(23) |
| C-$C_\alpha$ | 1.67(3) | 1.86(2) | 1.77(2) | 1.86(3) | 1.80(3) | 1.88(2) | 1.69(2) | 1.76 | 1.78 | 1.79(7) |
| | −8.6(1) | −14.5(1) | −13.4(1) | −15.5(1) | −15.4(1) | −15.5(1) | −12.9(1) | −10.8 | −15.6 | −13.6(25) |
| $C_\beta$-$C_\beta$ | 1.83(3) | 1.68(2) | 1.79(2) | 1.77(3) | 1.80(3) | 1.66(2) | 1.61(2) | 1.67 | – | 1.73(8) |
| | −16.1(1) | −10.1(1) | −14.8(1) | −14.4(1) | −13.8(1) | −11.5(1) | −12.1(1) | −10.1 | – | −12.9(22) |

  1433-7851/99/3810-1398 $ 17.50+.50/0 *Angew. Chem. Int. Ed.* **1999**, *38*, No. 10

are easily detectable. As an example we show a relief plot of the negative Laplacian function in Figure 1 for the four amino acids. Its topology around the carboxylate group is in very good agreement for all amino acids. The distribution of $\nabla^2\rho(\mathbf{r})$ in the valence region, which corresponds to the Lewis electron pair model and the VSEPR model of Gillespie,[3] allows an exact assignment of bonding and nonbonding electron pairs. All covalent bonds show the characteristic saddle-shaped bonding charge concentrations. The nonbonding charge concentrations of the oxygen atoms correspond to the lone pairs.

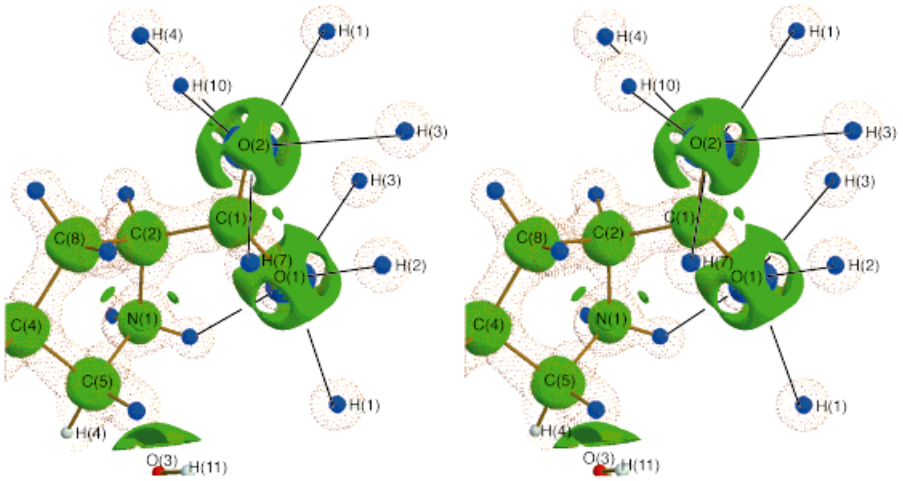


Figure 2. Stereo representation of three isosurfaces of the Laplacian function of DL-proline. Blue = 100 e Å$^{-5}$, red dots = zero surface, green = $-12$ e Å$^{-5}$. In addition to the proline molecule all hydrogen atoms that are involved in intermolecular hydrogen bonds are drawn. All connecting vectors from the oxygen atoms to these hydrogen atoms pass through regions of local charge concentration, which can be seen as holes in the green isosurface.

Quantitative values for $\rho(\mathbf{r})$ and $\nabla^2\rho(\mathbf{r})$ at the bond critical point, which give hints on the character and strength of a bond, are compiled in Table 2 for comparable bonds of the amino acids under investigation. The observed variations for a given bond in the range of 1–5 % for $\rho(\mathbf{r})$ and 7–19 % for $\nabla^2\rho(\mathbf{r})$ are even lower than those seen with Hartree–Fock calculations obtained from different basis sets.[9, 12] This means that especially for $\rho(\mathbf{r})$ a high degree of reproducibility and transferability is observable in this group of the amino acids. The bigger variation for $\nabla^2\rho(\mathbf{r})$ is not too surprising since it is the second derivative of the charge density and therefore much more sensitive to the curvature at the critical point. The various C–O bonds in the amino acids allows them to be compared quantitatively. In the carboxylate group, common to all compounds, we find mean values for $\rho(\mathbf{r})$ of 2.69/2.82 e Å$^{-3}$ at the bond critical points. For the C–O(H) bond of the hydroxyl group in Ser and Thr $\rho(\mathbf{r})$ is in the range of 1.81–1.85 e Å$^{-3}$. In the carboxyl groups (Glu and Asp) we find values of 2.21 and 2.41 e Å$^{-3}$ for $\rho(\mathbf{r})$ at the C–O(H) bond, whereas for the C=O bonds these values are 3.06 and 2.96 e Å$^{-3}$. For the C=O bond in Asn we find $\rho(\mathbf{r})$ = 2.89 e Å$^{-3}$. The comparison of these values, which describe the bond strength quantitatively, with values from some oligopeptides we are currently working on, should show how far they change on forming a peptide bond and how the transferability to peptides is expressed.

The three-dimensional distribution of the Laplacian function, which we generated from the proline data measured earlier, contains important information about weak interactions. According to Bader's theory local charge accumulation corresponds to strongly negative regions in the Laplacian function. These are visible as holes in the green isosurface for $\nabla^2\rho = -12$ e Å$^{-5}$ in the environment of the two oxygen atoms displayed in Figure 2. If the oxygen atoms are connected to the H atoms of their intra- and intermolecular hydrogen bonding partners, it is interesting to note that each of these connecting vectors passes through one of these holes as can easily be seen in the stereo representation of Figure 2. Thus the Laplacian function also describes fine charge-density reorganizations as a result of nonbonding interactions. Therefore, the directions where chemical interactions are favored can be observed from its topology.

The electrostatic potential (EP)[14] displayed in Figure 3 considers an isolated molecule extracted from the crystal but which still bears the polarization effects induced by intermolecular interactions. Thus a three-dimensional distribution of the EP in the crystal is obtained. This chemical environment surely simulates better, for example, physiological conditions, than an EP extracted from an isolated molecule, which is the situation most often considered in quantum chemical calculations. The EP not only plays an important role in the treatment of chemical reactivity but also when considering molecular recognition (for example, drug receptor interaction). This is because electrostatic forces are long-range interactions and therefore determine the reaction path of two molecules.

The isosurface representations in Figure 3 all show a big kidney-shaped electronegative region as a common feature around the carboxylate group. This region is more extended relative to electrostatic potentials derived from theoretical calculations,[5, 12] and we attribute this to polarization effects arising from intermolecular interactions in the crystal.

The following aspects seem important in regard to the above results: Thanks to fast experiments we were able to obtain comparable quantitative results on an electronic level for a number of amino acids. Similarity and molecular recognition play an important role in molecular modelling. The Laplacian function of a compound, which is now obtainable in a fast and reliable way with modern experimental methods, considers both aspects. The method used here yields the topology of the charge density in the crystalline state. In this state, in which molecular recognition is realized to a high degree, the derived properties of a system are surely closer to the "real" properties than those derived from the isolated stationary state. If it turns out that the functionality given by the Laplacian function is invariant with

  1433-7851/99/3810-1399 $ 17.50+.50/0 

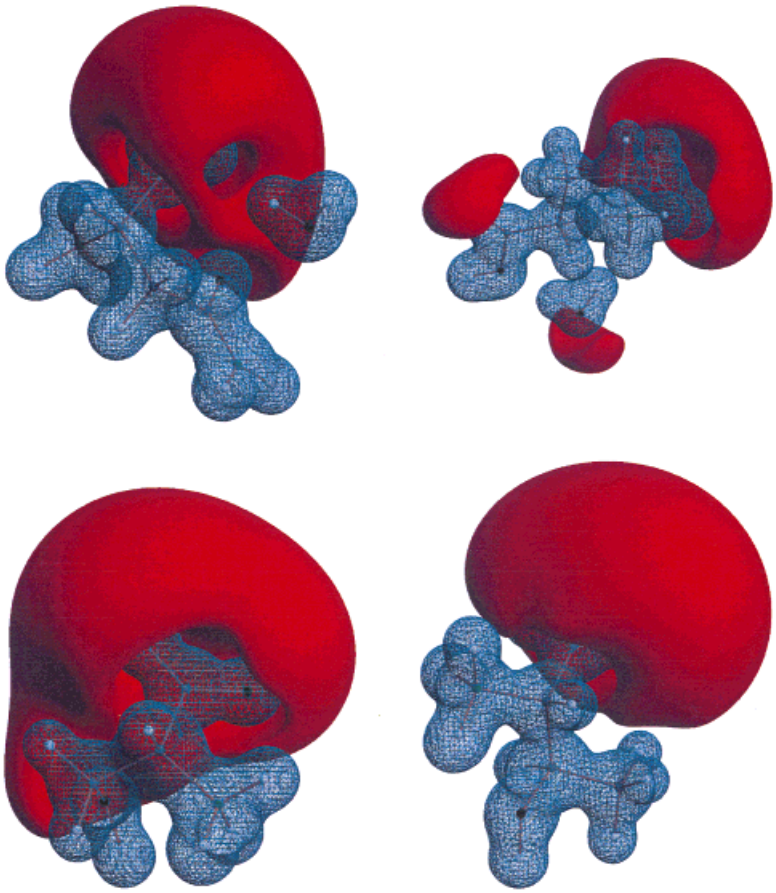

Figure 3. Isosurface representation of the experimental electrostatic potentials. Blue: positive potential, red: negative potential, L-Asn (top left, 0.5/ – 0.15), DL-Glu (top right, 0.5/ – 0.08), DL-Ser (bottom left, 0.5/ – 0.1), L-Thr (bottom right, 0.5/ – 0.1). Unit: e Å$^{-1}$.

respect to changing chemical environments (for example different crystal fields) then the behavior of a molecule in different chemical environments can be reliably predicted. Although atomic properties based on Bader's partitioning of the charge density were not determined, the similarity of the topology of chemically equivalent bonds found in this study yields an indirect proof for the transferability of atomic and group properties. The experimental determination of such properties will surely gain importance in the fields of molecular modelling and design as well as in crystal engineering.[15]

Received: December 10, 1998 [Z12768IE]
German version: *Angew. Chem.* **1999**, *111*, 1494 – 1497

**Keywords:** amino acids · charge density · electrostatic interactions · synchrotron radiation · topological analysis

[1] P. Coppens, *X-ray Charge Densities and Chemical Bonding*, Oxford Science Publications, **1997**.
[2] P. Coppens, *Science* **1967**, *158*, 1577; R. F. Stewart, *J. Chem. Phys.* **1969**, *51*, 4569.
[3] R. F. W. Bader, *Atoms in Molecules, A Quantum Theory*, Clarendon, Oxford **1990**; R. F. W. Bader, P. Lode, A. Popelier, T. A. Keith, *Angew. Chem.* **1994**, *106*, 647; *Angew. Chem. Int. Ed.* Engl. **1994**, *33*, 620.
[4] T. Koritsánszky, S. Howard, T. Richter, Z. W. Su, P. R. Mallinson, N. K. Hansen, *XD—A Computer Program Package for Multipole Refinement and Analysis of Electron Densities from Diffraction Data. User Manual*, Freie Universität Berlin, **1995**.
[5] T. Koritsánszky, R. Flaig, D. Zobel, H.-G. Krane, W. Morgenroth, P. Luger, *Science* **1998**, *279*, 356.
[6] C. Chang, R. F. W. Bader, *J. Phys. Chem.* **1992**, *96*, 1654.
[7] The synchrotron experiments were carried out at the beamlines D3 (four circle Eulerian cradle) and F1 ($\kappa$-axis geometry) at Hasylab/DESY. A Bruker CCD area detector and Oxford Cryosystem $N_2$ gas stream device were used. The measurement strategy was determined with ASTRO,[17] the measurement was controlled with SMART,[17] and the integration and correction of the data was done with SAINT[17] and SADABS.[18] Multipole refinements according to the formalism of Hansen – Coppens[16] were carried out with the program system XD[4] developed in our group. Hexadecapoles were used for the heavy atoms and dipoles (in a few cases quadrupoles) for the H atoms. The topological analysis, derivation of electronic properties, and graphical visualization (Figures 1 – 3) were also done with XD.
[8] An additonal measurement was performed on DL-serine with $Mo_{K\alpha}$ radiation; in the case of L-threonine the conventional point (scintillation) detection technique was used (see Table 1).
[9] C. Gatti, R. Bianchi, R. Destro, F. Merati, *J. Mol. Struc. (Theochem.)* **1992**, *255*, 409.
[10] R. Destro, R. Marsh, personal communication, **1998**.
[11] M. Carducci, R. Bolotovsky, P. Coppens, *Acta Crystallogr. Sect. A* **1996**, *52*, C342.
[12] R. Flaig, T. Koritsánszky, D. Zobel, P. Luger, *J. Am. Chem. Soc.* **1998**, *120*, 2227.
[13] The Laplacian function [Eq. (1)] is defined as the trace of the Hessian matrix of the charge density $\rho(\mathbf{r})$.

$$\nabla^2\rho(\mathbf{r}) = \frac{\partial^2\rho(\mathbf{r})}{\partial x^2} + \frac{\partial^2\rho(\mathbf{r})}{\partial y^2} + \frac{\partial^2\rho(\mathbf{r})}{\partial z^2} \quad (1)$$

[14] Z. W. Su, P. Coppens, *Acta Crystallogr. Sect. A* **1992**, *48*, 188.
[15] J. J. McKinnon, A. S. Mitchell, M. A. Spackman, *Chem. Eur. J.* **1998**, *4*, 2136.
[16] N. K. Hansen, P. Coppens, *Acta Crystallogr. Sect. A* **1978**, *34*, 909.
[17] Programme ASTRO 1995 – 1996, SMART 1996, SAINT 1994 – 1996, Bruker-AXS Inc., Madison, WI (USA).
[18] R. H. Blessing, *Acta Crystallogr. Sect. A* **1995**, *51*, 33.

  1433-7851/99/3810-1400 $ 17.50+.50/0 